Proceedings of the 11th International Symposium on Unmanned Untethered Submersible Technology, 1999, Pp. 378-388.

SWIMMING FISH AND FISH-LIKE MODELS: THE HARMONIC STRUCTURE OF UNDULATORY WAVES SUGGESTS THAT FISH ACTIVELY TUNE THEIR BODIES

Robert G. Root[1], Hayden-William Courtland[2], Charles A. Pell[3], Brett Hobson[3], Eamon J. Twohig[2], Robert B. Suter[2], William R. Shepherd III[2] , Nicholas C. Boetticher[2] and John H. Long, Jr.[2]

[1] Dept. of Mathematics, Lafayette College, Easton, PA, 18042,
(610) 250-5280 voice, robroot@cs.lafayette.edu

[2] Dept. of Biology, Vassar College, Poughkeepsie, NY, 12604,
(914) 437-7305 voice, (914) 437-7315 fax,
hacourtland99@alumn.vassar.edu, eatwohig@vassar.edu, suter@vassar.edu, jolong@vassar.edu

[3] Nekton Technologies, Inc., 710 West Main Street, Durham, NC 27701,
(919) 682-3993 voice, (919) 682-8779 fax, cap@ntrobotics.com, bhobson@ntrobotics.com

Abstract

To evaluate the versimilitude of theoretical and mechanical models of fish and fish-like propulsive systems, we compared quantitatively the motion of undulatory body waves using a Fourier-based method. The undulatory motions of a freely-swimming lamprey were compared to a series of theoretical and physical models. For each swimming trial, Fourier series of up to five frequencies were fit to the *x* (axial) and *y* (lateral) motion of 31 points reconstructed along the midline of each fish or model. Using a multiple regression technique, only frequencies that significantly ($p \leq 0.05$) described the axial and lateral displacements were included as explanatory variables. We found that models of all types, and backward-swimming lamprey, undulate with harmonics of higher-order than the fundamental frequency and 1st harmonic in lateral and axial motion, respectively. In contrast, the forward-swimming lamprey has far fewer higher-order harmonics. Since higher-order harmonics produce point trajectories that are kinematically complex and energetically costly, forward-swimming lamprey have sufficient mechanical motivation to swim in a manner consistent with the hypothesis that fish are able to actively tune their bodies in order to either suppress or remove higher harmonics from their undulatory wave motion.

Introduction

Using the body as a propeller, most fish swim using undulations, flexural body waves that travel from head to tail. This propulsive wave of motion, often over-simplified as a sinusoidal wave of constant or linearly-increasing lateral amplitude, is geometrically complex, with midline flexion accelerating faster than the lateral motion (Cheng et al. 1998; Katz & Shadwick, 1998; Jayne & Lauder, 1995) and axial motions producing figures-of-eight trajectories at the tail (Bainbridge, 1963). Consequently, the kinematic complexity of undulatory swimming has not been accurately and quantitatively described. Only with the proper analytic tool can we measure — and thus compare — the performance of swimming fish with the theoretical and mechanical models of fish-like swimmers currently being produced (Carling et al. 1998; Ekeberg, 1993; Librizzi et al, In press; McHenry et al. 1995; Root & Long, 1997). To develop this tool, and to test its accuracy and usefulness on fish and fish-like models, is the goal of this study.

Given that the wave motions of a steadily-swimming fish are periodic (Long et al. 1997), a Fourier-based analysis, in which periodic motion is decomposed into its harmonic constituents, was deemed appropriate. While Fourier-based methods have been employed previously (Videler & Hess, 1984), we sought to include, in addition to lateral motion, (1) axial motion and (2) a statistical basis for the inclusion or exclusion of harmonics.

Studies of whole-body kinematics and muscle activation serve as the basis for many theoretical models. In an attempt to mechanically model undulatory swimmers, researchers have employed two general approaches: (1) neurobiological models based on coupled neural oscillations directed by the central pattern generator and (2) dynamic bending models based on fundamental mechanical principles and hydrodynamic considerations. Some of the most important neurobiological studies were performed using the marine lamprey, and for that reason we use lamprey in this study. By developing interaction schemes for different locomotor neurons, computer simulations have demonstrated signal patterns which closely mimic the lamprey's neural activity (Grillner et al., 1993; Grillner et al. 1995). Ekeberg (1993) extended these models by simulating a mechanical environment in which an attached neural network could function. The results of this study have suggested that the neural control circuits charted by Grillner and others are sufficient in describing the motion of intact lamprey. Beginning instead with the mechanical principles governing motion, recent developments have modeled undulatory swimmers as continuous, dynamically-bending beams (Cheng et al. 1994; Cheng et al. 1998). In addition, the importance of whole-body accelerations, viscous forces, and rotational forces has been presented within the context of a two-dimensional undulatory model (Carling et al. 1998).

A central difficulty is faced by all models of undulatory swimming, whether they are neurobiological, mechanical or theoretical — how does the investigator know if, and to what degree, the model mimics the undulatory motion of the biological system? Studies of whole-body kinematics and other *in vivo* parameters give detailed descriptions which establish apparently general similarities and differences among species, but comparisons based on neuromechanical principles or mathematical representations are not easily derived from the resulting data. Descriptive models, on the other hand, are versatile in their predictive capabilities, but are severely limited by the assumptions made and by the often unnatural physical restraints placed on the model. For example, negligible axial motions, simple sinusoidal motion in the lateral dimension, and phase constraints have been employed throughout the literature (Videler & Hess, 1984; Grillner et al. 1995; Gillis, 1998). These simplifications mask many of the underlying subtleties that are vital to our understanding of undulatory swimming maneuvers.

In this paper we fit Fourier series of statistically-determined harmonics to undulatory motions, thereby mathematically describing the motions that characterize steady swimming in fish and fish-like models. In addition, we analyze and compare the motions of real fish to those of theoretical and mechanical models and find, to our surprise, that forward-swimming lamprey lack many of the higher-order harmonics seen in models and backward-swimming lamprey. This simpler harmonic structure suggests that forward-swimming lamprey are actively (*i.e.*, muscularly) tuning their undulatory motion in order to suppress or remove higher-order harmonics.

We chose specific models and behaviors in order to address the following questions (relevant models or behaviors are given parenthetically and discussed in detail in the Methods section):

1. How accurately does the Fourier-based method reconstruct undulatory motion?
   (theoretical kinematic models)
2. What is the harmonic structure of the undulatory motion generated by a traveling wave of sinusoidal lateral displacement or sinusoidal midline flexion?
   (theoretical kinematic models)
3. Do theoretical and mechanical models driven by internal forces in a fluid produce undulatory motion with harmonic structure different from that produced by sinusoidal waves?
   (theoretical plate model and mechanical oscillatory impellers)
4. Do swimming fish produce an undulatory motion with harmonic structure different from that produced by theoretical and mechanical models?
   (forward and backward-swimming lamprey)
5. Do swimming fish modulate the harmonic structure of their undulatory motion in order to produce different propulsive maneuvers?
   (forward and backward-swimming lamprey)

Materials and Methods

Models and Animals

Theoretical models. We present four different theoretical models: (1) a continuous constant-length midline with a sinusoidal wave of constant lateral amplitude (10% of total body length, *L*) traveling at constant velocity, (2) a midline with 30 segments with a wave of sinusoidally varying joint flexion (increasing exponentially from head to tail; values from Gillis, 1998) traveling at constant velocity, (3) a midline with 30 segments with a wave of sinusoidally varying joint flexion (increasing exponentially from head to tail) traveling with accelerating velocity (value from Katz & Shadwick, 1998), and (4) a continuous elastic plate with internal force generation ("muscles") and simple viscosity externally (Librizzi et al. In press). Please note that the first three of these models are kinematic only; *i.e.*, motion is modeled without reference to internal or external forces. These kinematic models shared several features — the head oscillated laterally but not axially and body length, *L*, was held constant.

The elastic plate model is a numerical implementation of an initial-boundary value problem for a fourth-order hyperbolic partial differential equation described in detail elsewhere (Librizzi, et al., In Press; Root & Long, 1997). The modeled fish was 20 cm in length with a maximum thickness of 1 cm and a maximum depth of 5 cm. The Young's modulus, *E*, of the body was 0.18 MPa, based on bending tests of sunfish (Long et al. 1994) and gar (Long et al. 1996); for the model, the head was assumed to be five times as stiff as the body. The muscle stresses never exceeded 15% of the maximum of 1.5×10^7 N m^{-2} per fiber as measured by Altringham et al. (1993). The muscles were activated in a sinusoidal pattern with a wavelength of 8 cm and a frequency of 3.7 Hz. This model's two most important limitations are the omission of inertial fluid forces acting on the fish (only viscous damping is used), and the modeling of the fish's body as perfectly elastic.

Mechanical models. Two three-dimensional Nektors™ (oscillatory impellers) were created at Nekton Technologies, Inc. using a polyurethane casting molded into a 14 cm long fish-like body. The models, of identical shape, varied in material stiffness, with the stiff Nektor™ having an *E* of 15.5 MPa and the flexible Nektor™ having an *E* of 5.5 MPa; modulus was measured using a Shore A hardness durometer (model 306L, Pacific Transducer Corp.). Analogous to our previous method (McHenry et al. 1995), the models were actuated to swim at a constant velocity (net thrust = net drag) in a water tunnel by way of a steel drive shaft cast within the model at approximately 0.2 L driven by an oscillating couple from computer-driven servomotor (model 630, brushless DC, Compumotor). During swimming, the shaft was permitted to move laterally and axially. Nektors™ were driven at a frequency of 12 Hz and a couple amplitude of ± 20°, conditions that generated traveling waves of flexures and, hence, undulatory locomotion. Nektor™ swimming was captured ventrally at 250 images per second (ips) using high-speed video (model 1000, Red Lake) with images captured from a mirror angled 45° to the bottom of the water tunnel.

Lamprey. The parasitic phase sea lamprey, *Petromyzon marinus* (*L* = 14.1 cm) used in this study was one of several obtained from the Lake Huron Biological Station in Millersburg, Michigan and was housed at 20 °C in an 80 L aquarium at Vassar College. Forward and backward swimming trials were recorded using high-speed video (Kodak model Ektapro 1000; 500 or 1000 ips). Sequences of volitional swimming were captured in a still-water aquarium and ranged in swimming speeds from 0.164 to 2.844 body L/s^{-1}. During filming, lamprey were backlit by a 500–watt halogen light diffused through a sheet of 0.5 cm white acrylic in order to capture clear, high contrast images. The ventral surface of each fish was taped by reflecting the light path off of a mirror located at an angle of 45° to the tank's bottom. Backward swimming in lamprey was initiated by gently approaching or stimulating the rostral end of the fish with a rubber tipped rod. Forward swimming was initiated by applying a similar stimulus to the caudal end. Only swimming sequences where the fish swam in a straight line at nearly constant velocity with the trailing edge

passing through a minimum of two opposite lateral extremes were used for kinematic measurements.

Digitizing and midline reconstruction

Video sequences for lamprey and Nektor™ trials were digitized using a video deck (model SVO-9500MD, Sony Corp.) linked to a computer (model Macintosh IIfx, Apple Corp.). A 10 x 10 cm square grid was placed in the video field for calibration of the digitized image. Using a video genlock (model Televeyes Pro, Digital Vision Inc.), the digitally frozen image was overlaid on the computer screen, which contained an *x,y* coordinate grid (Image software version 1.51, NIH). For the slender lamprey, a series of 20 points was manually plotted on the fish's midline for 15-30 frames per tailbeat cycle (see Long et al. 1997); the midline was estimated on screen as the point at a given position equidistant from the left and right sides of the fish. Since the body of a Nektor™ tapers substantially, we could not, using the method described for lamprey, reliably digitize the midline; instead we selected 20 points along each side of the Nektor™. A custom video digitizing program (Jayne & Lauder, 1993) was used to reconstruct a midline of nearly equal sized segments from the digitized data. For each digitized image, the program employed custom spline fitting to reconstruct a midline with 30 body segments (31 *x*,*y* body points).

Preliminary Fourier transforms

Midlines from fish and models were read into a custom Mathematica program (FishFourier) for analysis. To begin, a series of fast Fourier transforms (FFT) for each of the 31 body points identified frequency components constituting the continuous waveform of undulatory locomotion. These transforms, and all subsequent analyses, were conducted separately for *x* and *y* coordinate data in order to elucidate and verify their unique contributions to the overall motion. Transforms were windowed, selecting for frequencies smaller than twice an estimated tailbeat frequency (visual inspection) to prevent aliasing. The linear portion of the data, *i.e.*, constant velocity motion, was fit by least-squares at each body point and extracted from the FFT, leaving a *filtered Fourier transform* (or fFt), which represents the lamprey's periodic motion and acceleration. Velocities were then computed vectorially from every point's fFt and averaged to give the composite velocity vector, *s*, of each lamprey trial. Within each trial's analysis, the magnitude and direction of *s* never varied by more than 1% and 2°, respectively. The frequency and amplitude of the maximum-amplitude frequency (fundamental frequency, f_1) in the window were found for every body point in each trial's fFt. Frequencies were then averaged using the amplitudes as weights and the tailbeat period was calculated to the nearest multiple of the interframe time. Following the removal of constant velocity motion and the determination of the tailbeat period, a coordinate transformation was performed on the *x*, *y* position data to yield a coordinate system in the fish's frame of reference; that is, the positive *x*-axis points in the direction of the fish's progression. This transformation applied a rotation matrix to each *x*, *y* data pair yielding the respectively transformed coordinates pairs *u* and *v*.

Fourier fitting

Having established a tailbeat period and average velocity for the fish, the displacements were modeled with Fourier series. In order to determine the smallest set of Fourier harmonics that accurately predict the separate behavior of *u* and *v* data, we performed a forward selection multiple regression (Sokal & Rohlf, 1981), modified for our particular situation. In the standard forward selection procedure, the order in which the independent, or predictor, variables are introduced into the model depends on either the strength of their partial correlation or ability to significantly increase the coefficient of determination (r^2 value). Because our predictor variables are the individual Fourier frequency functions we had an *a priori* reason to believe that contribution of each frequency to the coefficient of determination would decrease with increasing frequency; *i.e.*,

the effects of the fundamental frequency, which corresponds to the tailbeat frequency in the lateral direction, are expected to dominate. Thus, harmonics were added in order of increasing frequency. Notice that this procedure thus provides a conservative test of the hypothesis that frequencies other than the fundamental are important in predicting undulatory motion.

To begin the fitting, the first tailbeat cycle of each trial was fit with a series of u, v regressions to determine statistically-significant components of the undulatory motion. The first regression gave the best fit linear function for both the u and v coordinates. For each coordinate independently, it uses the F-statistic for the model to determine whether the fit is statistically significant, using a specified threshold p-value (0.05 for this study). If the fit is significant, then t is one of the fitting functions used; if not, then the analysis begins with only constant functions used in the fit. The analysis proceeds through all the harmonics of the tailbeat cycle, beginning with the fundamental, ω_1, and ending with the fifth, ω_5. For each harmonic, the cosine and sine are regressed against the functions already being used in the fit to determine the residuals. These constitute the components of the functions orthogonal to the fitting functions already being used. The residuals of the data (that is the component not already explained by the current fitting functions) are then regressed against the residuals of the cosine and sine. Using the F-statistic of this model and the same threshold p value as above, the significance of the fit is assessed. If it is statistically significant that the residuals of the data are fit by the components of the new harmonic independent of the current fitting functions, then the harmonic is added to the fitting functions. As with the linear regression, the fitting of the u and v coordinates of a point are done independently of one another to describe the kinematics of individual body points. Once all the specified harmonics have been tested, the data is regressed against the fitting functions to give the final result. The fits for a given body point's axial and lateral motion are represented as follows:

$$(1)\quad u_p \sim C_{p0} + C_{p1}t + \sum_i \alpha_{pi}(\cos(\omega_{pi}t + \phi_{pi})) \qquad \textit{axial, } u$$

$$(2)\quad v_p \sim D_{p0} + D_{p1}t + \sum_i \alpha_{pi}(\cos(\omega_{pi}t + \phi_{pi})) \qquad \textit{lateral, } v$$

In these equations, C_{p0} and D_{p0} are the initial average values for the pth point's u and v components, respectively. These Fourier expansions are not centered on a horizontal line, as is usual (Haberman, 1998); instead, the average position moves along a line with slope C_{p1} or D_{p1} for the u or v component of the pth point, respectively. Other than this linear displacement of the average position, the motion is assumed periodic, and — for the purposes of this paper — the period is the tailbeat period, T, which is the time required for one full oscillation of the trailing edge of the fish. By harmonic analysis we mean the description of this periodic motion as a sum of oscillations whose frequencies are integer multiples of the fundamental frequency $\omega_1 = 2\pi/T$. The higher frequency, $\omega_i = i\omega_1$, where i is an integer greater than 1, is called the $(i-1)$st harmonic. It is a well-known theorem that periodic motion can be described as an infinite sum of sines and cosines of these higher harmonics (Haberman, 1998). Rather than the usual presentation of the ith frequency component of the motion as $A_i\cos(\omega_i t) + B_i\sin(\omega_i t)$, we prefer to express the expansion in terms of cosine functions with amplitude and phase. This is equivalent to the usual presentation using the following relation. For the u components the relation is: $\alpha_i = \sqrt{A_i^2 + B_i^2}$ is the amplitude of the motion, and $\tan\phi = -\dfrac{B_i}{A_i}$. For v components, α corresponds to β, and ϕ corresponds to ψ; all these parameters are indexed on both the frequency (i) and the point (p) whose motion is described.

The above equations treat each of the thirty-one midline points as discrete entities. Consequently, the inclusion or exclusion of harmonics is based solely on the motion of the body

point being analyzed. This approach enables a point–by–point comparison of periodic motion along the length of the fish appropriate for elucidating the role of localized variation in generating whole-body swimming motions.

In our analysis, we have not treated the infinite sequence of higher harmonic frequencies required by the mathematical theory; we truncated the higher harmonics at the fourth — five times the fundamental frequency. While our choice of the fourth harmonic was heuristic, it is clear from energetic considerations that the motion of the fish cannot have large amplitude motions at high harmonics. To see this, note that the energy required over a time interval is the integral of the power expended over the interval, and the power is the product of the force exerted and the velocity of the segment. That is, for a small segment of the fish undergoing periodic rigid motion, the energy required for motion at the $(i - 1)$st harmonic is as follows:

$$(3)\quad E_i = \int_{t_0}^{t_1} mav\ dt = m\omega_i^2 A_i^3 \int_{t_0}^{t_1} \cos(\omega_i t + \phi_i)\sin(\omega_i t + \phi_i)\, dt$$

where m is the mass of the segment. Over an entire cycle at this harmonic, that is, if the time interval $t_1 - t_0$ has length T/i, the energy is zero, since the segment has performed a closed loop; no work is performed. However, over smaller intervals we can see that the energy required increases with the square of multiple of the fundamental, i^2, and with the square of the amplitude A_i^2. Consider the interval between $t_0 = \frac{\phi}{2i\omega}T$ and $t_1 = \frac{\pi - 2\phi}{4i\omega}T$ as an example of an interval with the maximum possible energy required. Using standard Calculus, one can compute the energy required over this interval to be $E_i = 2m\left(\frac{\pi}{T}\right)^2 i^2 A_i^2$. There are $2i$ such intervals in a tailbeat period, T. Since there are an infinite number of harmonics, the energy associated with the $(i - 1)$st harmonic must eventually grow small with increasing i, and simply to maintain a constant magnitude of energy the amplitude A_I must grow smaller on the order of $1/i$. In practice, the fourth harmonic appears infrequent in the motion of actual fish, and always with small amplitude. By truncating the series at this frequency, we lost no appreciable amount of the harmonic analysis's ability to reconstruct the motion.

Results

Steadily swimming fish-like models, oscillatory impellers, and lamprey all generate flexural waves whose motion is primarily the sum of the two-dimensional periodic motions at individual points (Fig. 1). The presence of harmonics, and their relative amplitude, varies as a function of the kind of swimmer (features of model or behavior of fish), the dimension (axial or lateral), and position on the body (Fig. 2). In response to the questions posed in the Introduction, specific results are presented below.

1. The Fourier-based technique is highly accurate. As measured by the coefficient of determination (r^2 value), the Fourier-based fitting of the harmonic structure of the axial and lateral motion of body points on undulatory models recovers nearly 100 % of the total variance in motion (Fig. 2, the first three of four theoretical models).

2. The harmonic structure of the undulatory motion generated a traveling wave of sinusoidal lateral displacement or sinusoidal midline flexion is dominated, in amplitude, by the fundamental frequency in v and the first harmonic in u (Fig. 2, first three of four models). Together, these two frequencies produce a figure-of-eight trajectory at any point (Fig.1). While this figure of eight is

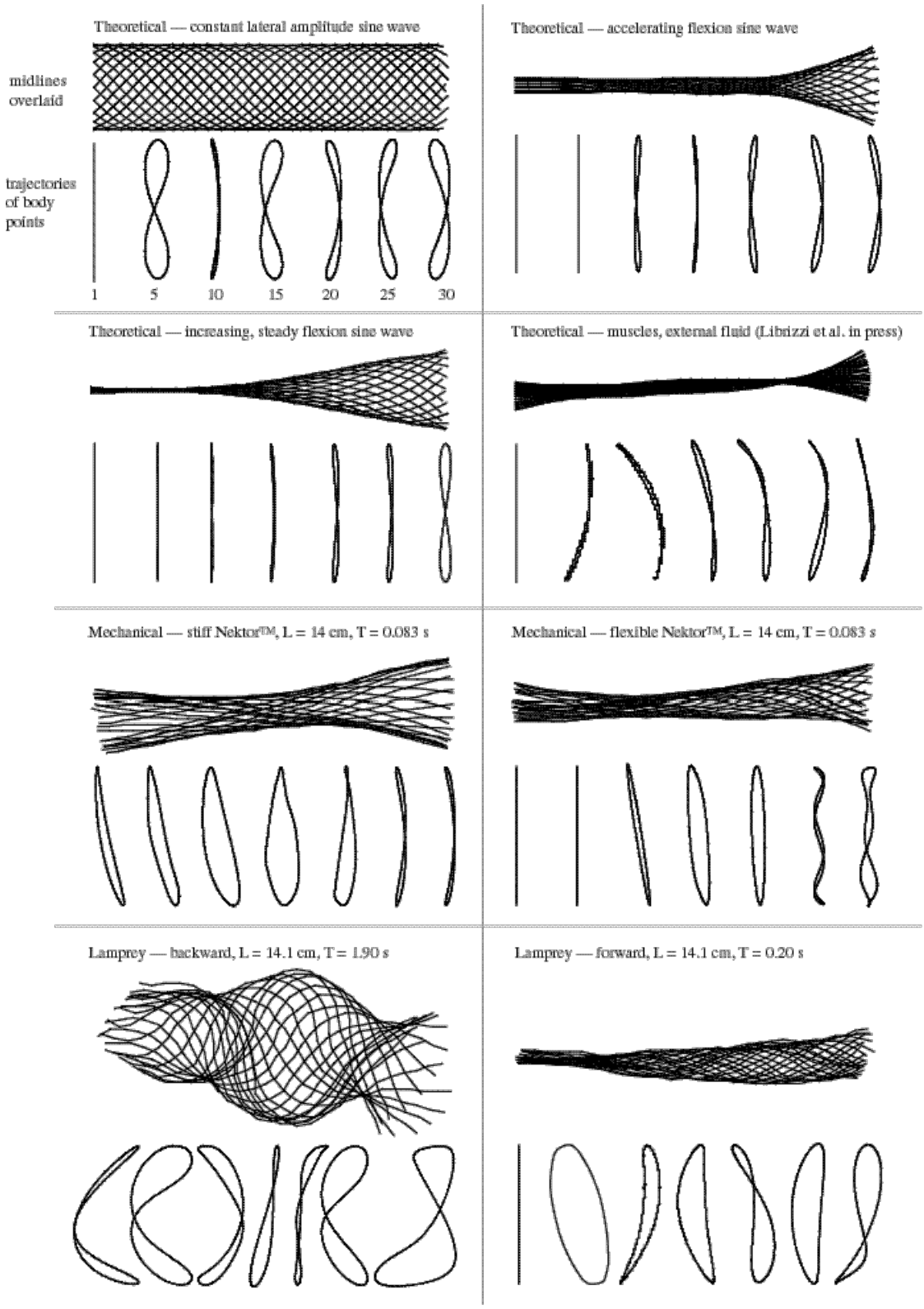

Figure 1. Midline kinematics of undulating fish-like models and lamprey (dorsal view, leading edge to right, one cycle). Midlines are reconstructed from digitized video (for Nektors™ and lamprey) using a custom program (Jayne & Lauder, 1993), and are shown with net translational velocity removed. Trajectories of body points are created using the Fourier-based method described in the text; note that the scales of the trajectories are proportionally expanded to permit comparison.

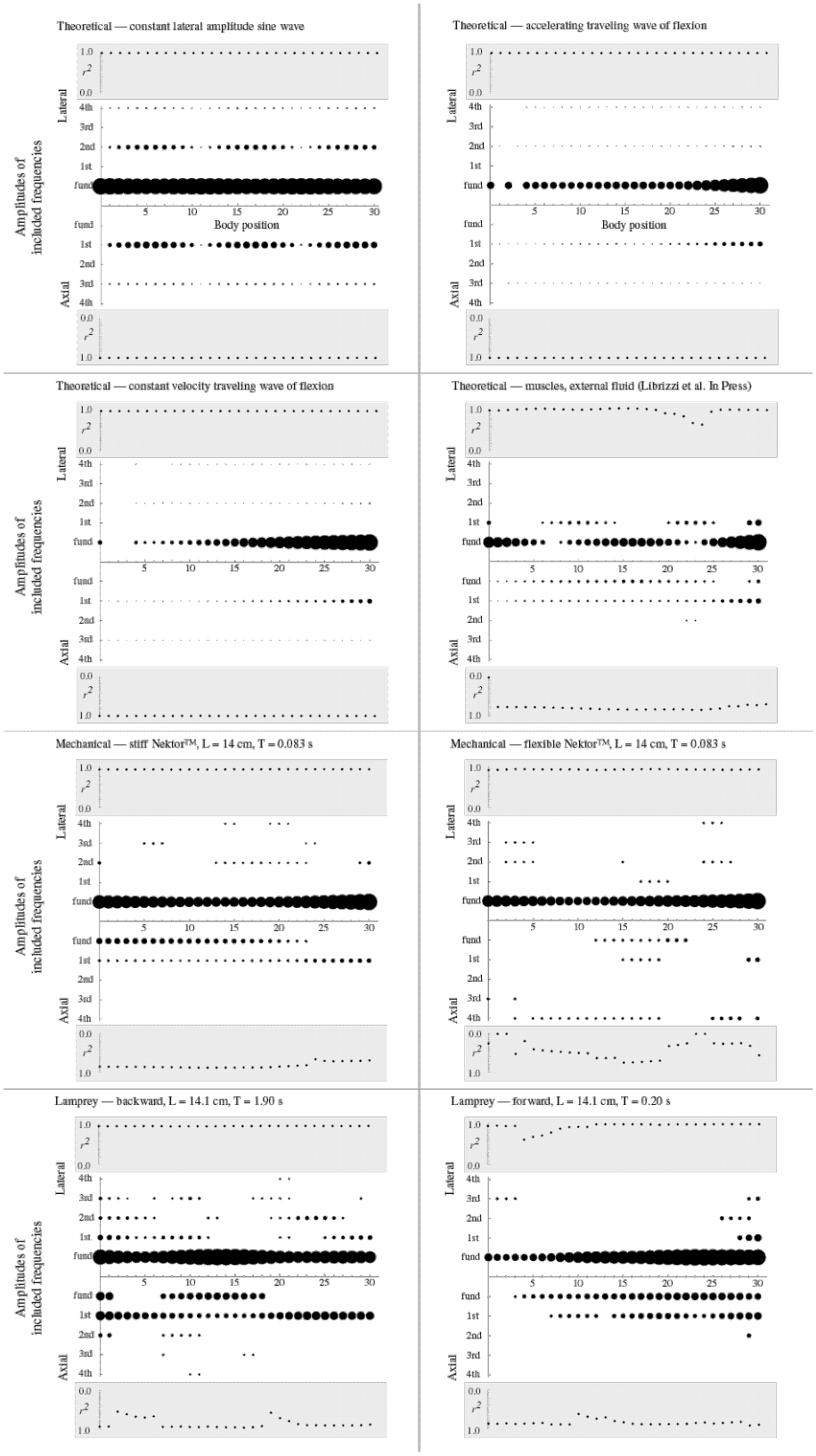

Figure 2. Harmonic structure of fish-like models and fish. Presence of a harmonic (significant at $p < 0.05$) is indicated by a black circle in the unshaded area; the area of the circle is proportional to the relative amplitude of that frequency. The goodness of the combined fit of all of the harmonics to the motion data at each point is indicated by the coefficient of determination (r^2) plotted in the shaded sections.

the predominant trajectory, the motion also contains higher-order harmonics in both dimensions (Fig. 2). Thus, a purely sinusoidal lateral or flexural input produces an undulatory wave having complex harmonic structure.

3. The theoretical model (Librizzi et al. In Press) and the mechanical impellers (Nektors™), which share the properties of having internal forces generating body waves that interact with external fluid forces, have wave motions with harmonic structure that differs from that seen in the theoretical kinematic models (Fig. 2). While the fundamental and 1st harmonic in *u* and *v*, respectively, are present in both kinds of models, the models with internal and external forces have higher harmonics present in a pattern different than that of the kinematic models. These different patterns are correlated with trajectories (Fig. 1) showing asymmetry and elliptical paths, in addition to figure-of-eight motions near the tail.

4. Lamprey swimming backward produce undulatory motion with harmonic structure that bears some resemblance to that of the stiff Nektor™, with the fundamental frequency present in *u* and *v*, the 1st harmonic present in *v*, and higher order harmonics in *v* (Fig. 2). Lamprey swimming forward, however, produce undulatory motion with harmonic structure that has only 13 higher-order harmonics (where higher-order refers to $\square_2$, $\square_3$, $\square_4$, and $\square_5$ in *v* and $\square_3$, $\square_4$, and $\square_5$ in *u*) in either dimension. The model with the next-lowest number of higher harmonics is the theoretical force model (Librizzi et al. In Press), which has 20.

5. When the lamprey swims backward, compared to swimming forward, it produces undulatory motion with almost four times the number of higher harmonics (68 v. 20, see Fig. 2).

Discussion

Higher-order harmonics, by which we mean those above the lateral fundamental and the axial 1st harmonic required to create a figure-of-eight trajectory, are present at most points of the body in the undulatory motion of all models and in backward-swimming lamprey (Fig. 2). Given the broad range of conditions represented by these models (Fig. 1) — simple traveling waves of lateral displacement or midline flexion; muscularly driven undulations; polyurethane impellers generating thrust in water — it is striking that forward-swimming lamprey completely lack higher-order harmonics in body points 4 to 25 (almost two-thirds of the body length). While only one trial is presented here, this general result holds for a sample size of 20 trials from seven lamprey (Root et al. In review).

What are the mechanical consequences of having fewer higher-order harmonics? Since the energy to move a segment periodically is proportional to the cube of the frequency under consideration (Eq. 3), higher-order harmonics require that the model or lamprey expend more energy to undulate. Compared to swimming backward, a forward swimming lamprey also has lower lateral amplitudes at most body points, a result similar to that found in forward and backward swimming eels, *Anguilla anguilla* (D'Aout & Aerts, 1999). As mentioned by D'Aout & Aerts (1999), higher amplitudes are energetically costly. In fact, the energy cost of motion is proportional to the square of the amplitude (Eq. 3). Hence, backward swimming, for both lamprey and eels, appears to be a far less energetically efficient mode of transport, especially when one considers the slow speed at which lamprey move backward (Fig. 1).

The presence of higher harmonics in backward-swimming lamprey and in the theoretical and mechanical undulators leads us to predict the following: *forward-swimming lamprey are actively tuning their bodies in order to suppress or remove higher-order harmonics.* This hypothesis is novel, and suggests to the engineer that biomimetic swimmers and oscillatory impellers will require mechanical filters and/or driver signal modulation in order to approach the energy efficiency and harmonic simplicity of forward-swimming lamprey.

How might lamprey actively tune their bodies? American eels, *Anguilla rostrata*, have the ability to triple the flexural stiffness of their bodies using their lateral body musculature (Long, 1998). By modulating body stiffness using muscles, fish could vary their natural frequency to reduce the moment needed to drive and propagate the traveling wave of bending (Long & Nipper, 1996). In addition, eels also possess the capacity to actively vary the body's damping coefficient by an order of magnitude (Long, 1998). Since damping moments absorb the kinetic energy of the traveling wave, damping coefficients could be actively tuned to attenuate the higher-frequency vibrations caused by the harmonics of undulatory motion.

It is also possible that lamprey suppress higher-order harmonics at the source of the undulatory signal. Since higher-order harmonics are generated from sinusoidal signals in the theoretical models (Fig. 2, first three of four theoretical models), source suppression would require non-sinusoidal signal generation. Non-sinusoidal periodic strain has been measured in the locomotor muscle of live milkfish, *Chanos chanos*, using implanted sonomicrometers (Katz et al. 1999). Since, under optimal conditions, muscles generate bending moments roughly in proportion to their strain rate or shortening velocity, it is possible that active tuning may be accomplished by signal suppression at the muscles.

In conclusion, we have presented a Fourier-based method that accurately describes the harmonic structure of the point-by-point periodic motions of undulating bodies. The isolated periodic motions are variants of a figure of eight (Fig. 1), a trajectory created by the presence of a fundamental frequency and 1st harmonic in the lateral and axial directions, respectively. In addition, most undulatory motion is characterized by the presence of harmonics higher than those just mentioned. That these higher-order harmonics appear in simple kinematic models (Fig. 2), would appear to require a new null hypothesis for undulatory motion — that undulatory motion is harmonically complex. Thus, when those higher-harmonics are missing — when undulatory motion is harmonically simple — mechanisms, heretofore unrecognized, must be at work to suppress or remove them. The mechanism we propose is that fish use their muscles to adaptively tune their bodies, changing flexural stiffness and damping to mechanically modulate the propagation of the traveling propulsive wave of bending.

Acknowledgements

This work was funded by ONR grants to RGR & JHL (ONR #N-00014-97-1-0292) and to CAP (ONR # N-00014-97-C-0462, Award: STTR Phase II). We wish to thank Jeff Cynx for his critical discussions of the analysis of harmonics.

References

Bainbridge, R. (1963). Caudal fin and body movement in the propulsion of some fish. *J. exp. Biol.* **40**, 23-56.

Carling, J., Williams, T.L., & Bowtell, G. (1998). Self-propelled anguilliform swimming: simultaneous solution of the two-dimensional Navier-Stokes equations and Newton's laws of motion. *J. Exp. Biol.* **201**, 3143-3166.

Cheng, J-Y. & Blickhan, R. (1994). Bending moment distribution along swimming fish. *J. Theor. Biol.* **168**, 337-348.

Cheng, J.-Y., Pedley, T.J. & Altringham, J.D. (1998). A continuous dynamic beam model for swimming fish. *Phil. Trans. R. Soc. Lond.* B **353**, 981-997.

D'Aout, K. & Aerts, P. (1999). A kinematic comparison of forward and backward swimming in the *eel Anguilla anguilla*. *J. exp. Biol.* **202**, 1511-1521.

Ekeberg, O. (1993). A combined neuronal and mechanical model of fish swimming. *Biol. Cybern.* **69,** 363-374.

Gillis, G.B. (1998). Environmental effects on undulatory locomotion in the american eel *Anguilla rostrata*: kinematics in water and on land. *J. Exp. Biol.* **201**, 949-961.

Grillner, S., Deliagina, T., Ekeberg, O., El Manira, A., Hill, R.H., Lansner, A., Orlovsky, G. N. & Wallen, P. (1995). Neural networks that co-ordinate locomotion and body orientation in lamprey. *Trends Neourosci.* **18** (6), 270-279.

Grillner, S., Matsushima, T., Wadden, T., Tegn**e**r, J., El Marina, A. & Wall**e**n, P. (1993). The neurophysiological bases of undulatory locomotion in vertebrates. *Sem. Neurosci.* **5,** 17-27.

Haberman, R. (1998). *Elementary Partial Differential Equations*, 3rd ed. Prentice Hall, Englewood Cliffs, NJ.

Jayne, B.C. & Lauder, G.V. (1993). Red and white muscle activity and kinematics of the escape response of the bluegill sunfish during swimming. *Comp. Physiol. A.* **173**, 495-508.

Jayne, B.C. & Lauder, G.V. (1995). Speed effects on midline kinematics during steady undulatory swimming of largemouth bass, *Micropterus salmoides*. *J. exp. Biol.* **198**, 585-602.

Katz, S.L. & Shadwick, R.E. (1998). Curvature of swimming fish midlines as an index of muscle strain suggests swimming muscle produces net positive work. *J. theor. Biol.* **193**, 243-256.

Katz, S.L., Shadwick, R.E. & Rapaport, H.S. (1999). Muscle strain histories in swimming milkfish in steady and sprinting gaits. *J. exp. Biol.* **202**, 529-541.

Librizzi, N.N., Long, J.H. Jr. & Root, R.G. (In press). Modeling a swimming fish with an initial-boundary value problem: unsteady maneuvers of an elastic plate with internal force generation. *Comp. & Math. Modeling.*

Long, J.H. Jr. (1998). Muscles, elastic energy, and the dynamics of body stiffness in swimming eels. *Am. Zool.* **38**, 771-792.

Long, J.H. Jr., Hale, M.E., McHenry, M.J. & Westneat, M.W. (1996). Functions of fish skin: flexural stiffness and steady swimming of longnose gar *Lepisosteus osseus*. *J. exp. Biol.* **199**, 2139-2151.

Long, J.H. Jr., McHenry, M.J. & Boetticher, N.C. (1994). Undulatory swimming: how traveling waves are produced and modulated in sunfish (*Lepomis gibbosus*). *J. exp. Biol.* 192, 129-145.

Long, J.H. Jr. & Nipper, K.S. (1996). The importance of body stiffness in undulatory propulsion. *Am. Zool.* **36**, 678-694.

Long, J.H. Jr., Shepherd, W. & Root, R.G. (1997). Maneuverability and reversible propulsion: how eel-like fish swim forward and backward using traveling body waves. *Proc. 10th Intl. Symp. UUST, Spec. Ses. Bio-Eng.*, 118-134.

McHenry, M.J., Pell, C.A. & Long, J.H. Jr. (1995). Mechanical control of swimming speed: stiffness and axial waveform in undulating fish models. *J. exp. Biol.* **198**, 2293-2305.

Root, R.G. & Long, J.H. Jr. (1997). A virtual swimming fish: modeling carangiform fish locomotion using elastic plate theory. *Proc. 10th Intl. Symp. UUST, Spec. Ses. Bio-Eng.*, Suppl. 1-7.

Videler, J.J. and Hess, F. (1984). Fast continuous swimming of two pelagic predators, saithe (*Pollachius virens*) and mackerel (*Scomber scombrus*): a kinematic analysis. *J. exp. Biol.* **109,** 209-228.